

# Thermal response of a 4D carbon/carbon composite with volume ablation: a numerical simulation study

Bai Zhang<sup>1</sup>  · Xudong Li<sup>1</sup>

Received: 8 July 2017 / Accepted: 12 July 2017 / Published online: 28 July 2017  
© Springer Science+Business Media B.V. 2017

**Abstract** As carbon/carbon composites usually work at high temperature environments, material ablation inevitably occurs, which further affects the system stability and safety. In this paper, the thermal response of a thermoprotective four-directional carbon/carbon (4D C/C) composite is studied herein using a numerical model focusing on volume ablation. The model is based on energy- and mass-conservation principles as well as on the thermal decomposition equation of solid materials. The thermophysical properties of the C/C composite during the ablation process are calculated, and the thermal response during ablation, including temperature distribution, density, decomposition rate, char layer thickness, and mass loss, are quantitatively predicted. The present numerical study provides a fundamental understanding of the ablative mechanisms of a 4D C/C composite, serving as a reference and basis for further designs and optimizations of thermoprotective materials.

**Keywords** C/C composite · Numerical simulation · Thermophysical property · Volume ablation

## 1 Introduction

Thermal protection materials play an important role in shielding of interior structural components, such as rocket nozzles and nose tips of spaceplanes, in severe temperature environments. Carbon/carbon (C/C) composites are excellent advanced materials due to their outstanding thermophysical properties and size stability, and are amongst the most promising high temperature materials. Indeed, C/C composites are widely used as thermal protection materials and structural components for high temperature conditions [1–3]. Nevertheless, material ablation due to the complexity of thermochemical environments, wherein material structures undergo extremely high temperatures, remains a challenge to their application. Therefore, the study of their thermal response during the volume ablation process, albeit

---

✉ Xudong Li  
zb\_yhc@163.com

<sup>1</sup> State Key Laboratory of Advanced Processing and Recycling of Nonferrous Metals, Lanzhou University of Technology, Lanzhou 730050, China

complex, is important to calculate their working temperature range as well as to develop and optimize the structure of new thermal protection materials. In addition, an understanding of the ablation mechanism is key with regards to the design of thermal shield material structures.

The ablation of materials as well as the identification of the ablative mechanism have been the object of numerous works. Several previous studies have assessed the thermal ablation behavior and underlying mechanisms during the thermochemical erosion of nozzle throats in rocket motors [4–6], and provided good predictions of ablative surface recession and useful results of ablation surface morphology. Furthermore, mathematical models to reproduce the roughness of carbon-based composites undergoing ablation have also been reported [7–10]. These models applied a Hamilton–Jacobi equation to describe the propagation of the ablation surface and assumed that the velocity of surface recession at any point in the location depends on surface orientation and the rate of mass transfer. The models were able to accurately characterize the roughness morphology of the ablator during ablation. Moreover, further studies applied material response models to simulate the thermal response of porous materials [11–16], solving the volume-averaged forms of the governing equations for flow field and presenting the time-dependent mass fraction of the gas component. Additionally, a model was established to simulate the microscale ablation for low-density carbon fibers [17] based on high fidelity imaging of the material microstructure and focused on the consumption of fiber ablator under ablation conditions. Li et al. [18, 19] established the counterflow diffusion flame model to describe the combustion phenomena of pyrolysis gases in the boundary layer as well as a non-linear pyrolysis layer model to analyze the thermal response of the charring ablator [20, 21]. The latter model divided the ablator into different layers and the transient heat conduction equations, in various forms, were respectively solved in each layer; the thickness of each layer was estimated by moving the material interfaces between different layers. Similarly, Scoggins et al. [22, 23] proposed a pyrolysis interface model, consisting of char and virgin layers. The difference between Li et al.’s model [20, 21] and that of Scoggins et al. [22, 23] is that the latter regarded the pyrolysis zone, which was described as a layer in the former, as an interface of zero thickness. Additionally, a few previous works [24–27] have presented several numerical models. The heat conduction equation coupling Arrhenius’ law has been used to predict the mass flow of pyrolysis gases. Yin [28], Wang [29, 30], and Meng [31] applied multiphysics coupled methods to simulate the thermal response and ablative behavior of C/C composites. However, the thermal response calculation of solid structures only considered heat conduction without bearing in mind the influence of internal material decomposition. Although these methods provide thermal and ablation information, the mass loss and the effect of material decomposition on heat transfer in the volume ablation process are difficult to compute with such models.

The mathematical models and numerical methods described above can, to a certain extent, accurately predict the material ablation process. However, the matrix and fibers of the C/C composite have differing ablation characteristics, and these models and methods have not considered the thermal response of composite materials with complex structures, such as that of a four-directional (4D) C/C, during ablation. With this motivation, an ablative model is developed and utilized herein to study the thermal response of a thermoprotective 4D C/C composite in the volume ablation process. The model considers the thermophysical properties during ablation and simulates the thermal response of the matrix and fiber components of a 4D C/C composite.

## 2 Numerical model

### 2.1 Equations governing the ablation process

The ablation process of composites is a highly coupled process under high temperature environment, involving the transfer of energy and mass. Thus, the characterization of thermal response during ablation of the composite materials should consider the unsteady heat transfer, and the material thermal decomposition mainly occurring in the ablation process. Accordingly, the energy conservation equation must inevitably include the material decomposition process via source terms and state-dependent material properties. In order to facilitate the calculation, several assumptions are made herein to solve the heat and mass transfer issue. Firstly, the volatile gases only flow along the thickness direction ( $y$ -axis). Secondly, there is thermal equilibrium between the remaining solid materials and the volatile gases under ablation. Under these assumptions, in the orthogonal Cartesian coordinate system ( $x, y, z$ ), the non-linear energy and mass equations describing the ablation process and considering unidirectional flow of gases along the  $y$ -axis direction are given by [32–34]:

$$\rho C_p \frac{\partial T}{\partial t} = \frac{\partial}{\partial x} \left[ k \frac{\partial T}{\partial x} \right] + \frac{\partial}{\partial y} \left[ k \frac{\partial T}{\partial y} \right] + \frac{\partial}{\partial z} \left[ k \frac{\partial T}{\partial z} \right] - \dot{m}_g C_{pg} \frac{\partial T}{\partial y} + \Delta h \frac{\partial \rho}{\partial t} \quad (1)$$

$$\frac{\partial \dot{m}_g}{\partial y} = - \frac{\partial \rho}{\partial t} \quad (2)$$

where  $\rho$  is the material density,  $C_p$  is the specific heat capacity,  $T$  is the temperature,  $t$  is the time,  $k$  is the heat conductivity,  $C_{pg}$  is the heat capacity of the gases,  $\dot{m}_g$  is the mass flux, and  $\Delta h$  is the heat of decomposition per unit mass of gas produced at the local temperature.

Further, the term on the left-hand side of Eq. (1) gives the change of internal energy of the material. The first three terms on the right-hand side represent the heat conduction, while the remaining two terms correspond to the convective heat transport and the heat of material decomposition, respectively.

The associated boundary conditions for (1) can be defined according to energy balance on the heating surface. The expression is as follows:

$$q_N = q_{conv} + q_{rad-in} - q_{abl} - q_{rad-out} \quad (3)$$

where  $q_N$  is the conduction into the material,  $q_{conv}$  is the total convective heat flux,  $q_{rad-in}$  is the radiation into the structure's surface,  $q_{abl}$  is the heat removed by surface ablation, and  $q_{rad-out}$  is the radiation away from the structure's surface.

### 2.2 Thermal properties of the decomposing material

An exact prediction of the thermal behavior and decomposition process of a composite material is inseparable from its thermal and physical properties. These properties (e.g., density, thermal conductivity, and specific heat capacity) are used as input data for the equations governing the thermal response and ablation behavior of composite materials. The accuracy of these input data directly affects the validity of the thermal analysis prediction.

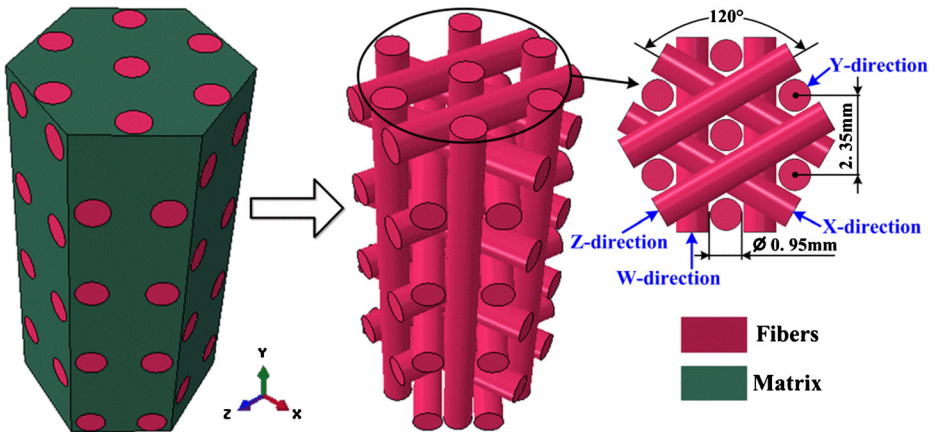


**Fig. 1** Geometry model of a 4D C/C composite

Composite material density varies significantly during the thermal decomposition process. Such a variation with time can be calculated using the first order decomposition equation. Thus, the composite density can be calculated as follows [32, 33]:

$$\frac{\partial \rho}{\partial t} = -(\rho_v - \rho_c) \left[ \frac{\rho - \rho_c}{\rho_v - \rho_c} \right]^n A e^{\left( \frac{-E}{RT} \right)} \tag{4}$$

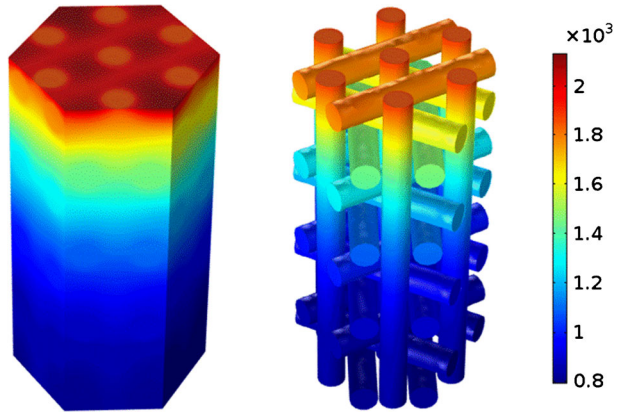
where A is the pre-exponential factor, E is the activation energy, R is the universal gas constant, and n is the order of reaction. Further,  $\rho_v$  and  $\rho_c$  represent the density of the virgin and decomposed (char) composites, respectively.

The thermophysical properties of the composite material undergo constant change during the gradual decomposition process. Prior to thermal decomposition, the material properties correspond to those of the virgin composite, while, following decomposition, they correspond to a fully decomposed (char) material. Thus, in order to obtain the intermediate state properties

**Table 1** Material properties of a 4D C/C composite

Name	Value	Unit
Fiber specific heat capacity	750	J/(Kg·K)
Fiber heat conductivity	22	W/(m·K)
Virgin material density	1298	Kg/m <sup>3</sup>
Decomposed material density	519	Kg/m <sup>3</sup>
Order of reaction	3	-
Pre-exponential factor for matrix	$9.75 \times 10^8$	s <sup>-1</sup>
Pre-exponential factor for fiber	$1.2 \times 10^7$	s <sup>-1</sup>
Activation energy for matrix	$1.7 \times 10^5$	kJ/mol
Activation energy for fiber	$1.33 \times 10^5$	kJ/mol
Universal gas constant	8.314	J/(mol·K)
Specific heat capacity of gases	$1159.406 + 4.323 T - 6.641 \times 10^{-4} T^2$	J/(Kg·K)
Heat of decomposition	$1.636 \times 10^6 - 2828.984 T + 4.705 T^2 - 8.347 \times 10^{-4} T^3$	J/Kg
Virgin material heat conductivity	$0.634 + 4.481 \times 10^{-6} T$	W/(m·K)
Decomposed material heat conductivity	$2.119 - 4.648 \times 10^{-4} T + 3.575 \times 10^{-7} T^2$	W/(m·K)
Virgin material specific heat capacity	$430.641 + 1.711 T - 8.234 \times 10^{-4} T^2 + 1.234 \times 10^{-7} T^3$	J/(Kg·K)
Decomposed material specific heat capacity	$338.739 + 1.493 T - 6.155 \times 10^{-4} T^2 + 8.273 \times 10^{-8} T^3$	J/(Kg·K)

**Fig. 2** Temperature distribution at an ablation time of 20 s



for thermal analysis, the properties of the decomposing composite are assumed to be dependent on the relative mass fractions of the virgin and fully decomposed materials. Several methods have been presented to calculate the thermophysical properties of materials under high temperature conditions [32–34]. Based on these methods, the mass fraction of the virgin material during the decomposing process can be defined as follows:

$$F = \frac{\rho - \rho_c}{\rho_v - \rho_c} \tag{5}$$

By using such a mass fraction as a progress variable representing the extent of material decomposition and associating it with other composite material properties, the thermal conductivity of the decomposing material can be defined as follows [32–34]:

$$k = F \cdot k_v(T) + (1-F) \cdot k_c(T) \tag{6}$$

Similarly, the specific heat capacity is defined by:

$$C_p = F \cdot C_{p(v)}(T) + (1-F) \cdot C_{p(c)}(T) \tag{7}$$

where  $k_v$  is the thermal conductivity of the virgin composite,  $k_c$  is the thermal conductivity of the decomposed (char) composite,  $C_{p(v)}$  is the specific heat capacity of the virgin composite,

**Fig. 3** Surface temperature as a function of ablation time

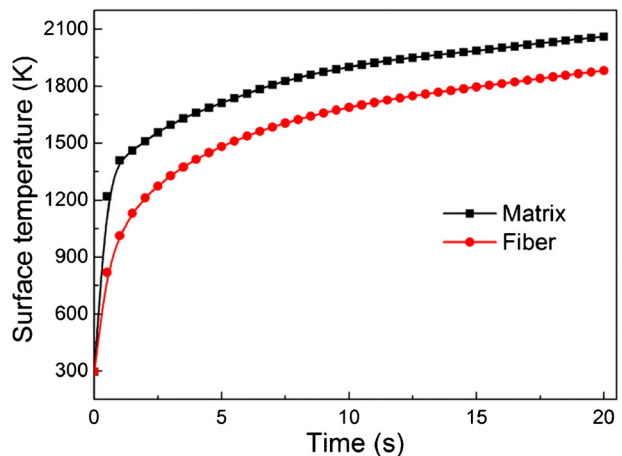
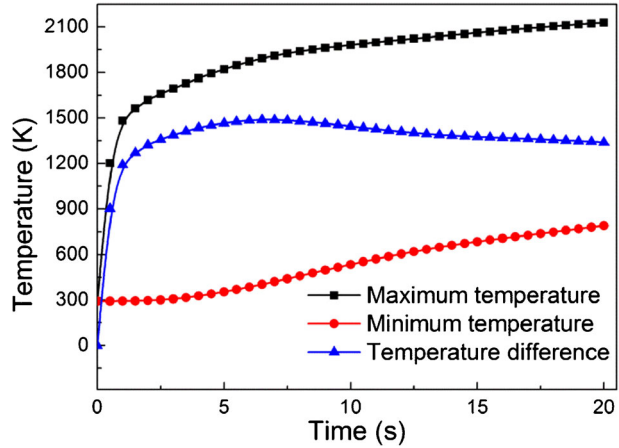


**Fig. 4** Maximum and minimum temperatures as a function of ablation time

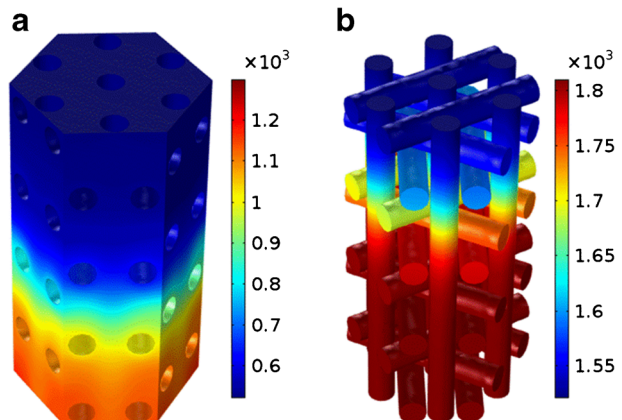


and  $C_{p(c)}$  is the specific heat capacity of the decomposed (char) composite. These parameters represent temperature-dependent variables in the analysis process.

### 3 Results and discussion

The above mentioned theory is used herein to analyze the thermal response of a thermoprotective 4D C/C composite. Fig. 1 shows a Representative Volume Element (RVE) as a computational domain including matrix and fibers. The fiber diameter is 0.95 mm and the material structure height is 12.4 mm. The thermal properties of the 4D C/C composite are listed in Table 1, while the remaining material parameters, including the fiber density, are obtained by the calculation process. During ablation, the top surface ( $y = 12.4$ ) of the C/C composite structure is exposed to high temperatures. On this surface, the thermal boundary condition is specified according to Eq. (3). With these conditions, the heat fluxes on the surface are taken as  $q_{com} = 2.8 \times 10^6 \text{ W/m}^2$  and  $q_{abl} = 51,900 \text{ W/m}^2$ . The radiation heat flux  $q_{rad-in}$  from the gas boundary layer into the material is not significant and is thus neglected. The emissivity for  $q_{rad-out}$  is set to 0.9. The bottom surface of the material structure is unexposed to the high temperature and a radiation boundary condition is specified on this surface, with an

**Fig. 5** Density distribution of (a) the matrix and (b) fibers at an ablation time of 20 s



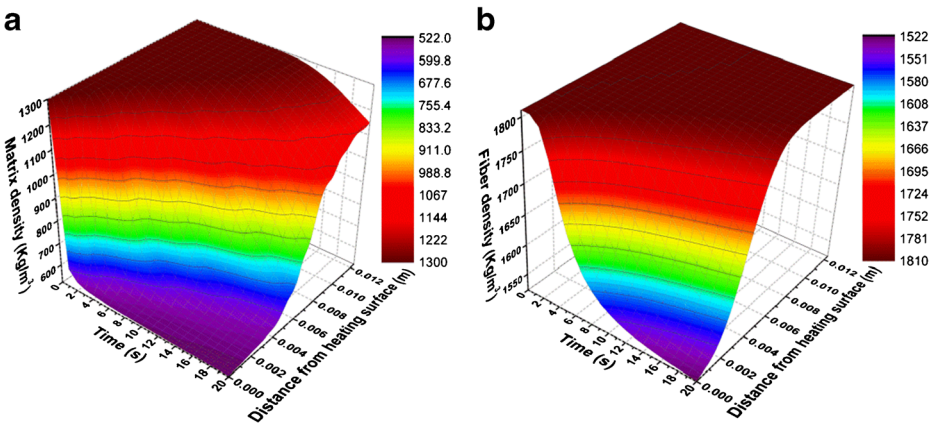


**Fig. 6** Density variation in (a) the matrix and (b) fibers with time and distance during ablation

emissivity of 0.5. Additionally, the boundaries for the remaining surface are considered to be adiabatic.

Fig. 2 shows the temperature distribution of the entire C/C composite and fibers during ablation for 20 s. The temperature distribution on the heating surface is not uneven, with the temperature gradually decreasing from top to bottom. The maximum surface temperature reaches 2129 K, and the temperature of the matrix on the heating surface is significantly higher than that of the fibers, with the temperature difference reaching 246 K. This effect is attributed to the much lower thermal conductivity of the matrix in relation to that of the fibers during ablation and the consequent concentration of heat on the matrix surface. Additionally, the temperature difference between the matrix and fibers in regions further from the heating surface is relatively small. A considerable temperature gradient is observed in the thickness direction of the material structure, with the maximum temperature difference reaching 1338 K at 20 s.

The surface temperature curves of the matrix and fibers in the C/C composite (Fig. 3) show a gradual increase in surface temperature with ablation time, while the temperature increment rate (i.e., the slope of the surface temperature curves) decreases with ablation time. Based on this, it is speculated that the surface temperature will reach a plateau, and that subsequent temperature changes will be observed mainly along the thickness direction of the structure

**Fig. 7** Average matrix and fiber densities as a function of ablation time

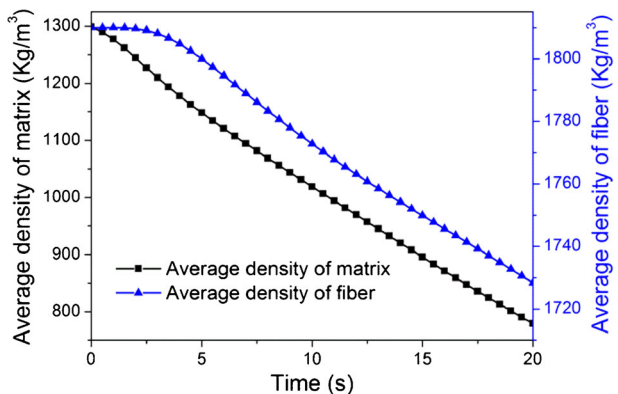
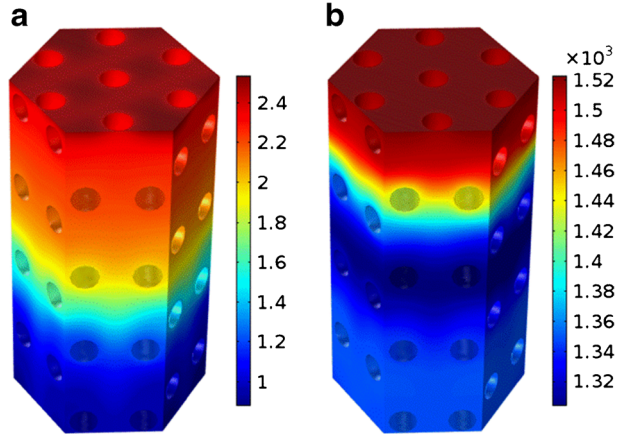


**Fig. 8** Thermal conductivity (a) and specific heat capacity (b) of the matrix at an ablation time of 20 s



upon increasing ablation time. Furthermore, as the ablation time increases, the surface temperature curves of the matrix and fibers synchronize, and the temperature difference between the matrix and fibers on the heating surface shows a decreasing tendency. At 20 s, the fiber temperature reaches 1883 K, 11.6% lower than the matrix temperature.

The maximum and minimum temperature of the C/C composite during ablation increase significantly with ablation time (Fig. 4). Conversely, the temperature difference between the maximum and minimum temperature gradually reduces with ablation time, indicating that, as the ablation process proceeds and ablation time is prolonged, the temperature of the material structure will equilibrate.

During ablation of the C/C composite, the density is observed to change constantly. The density distribution and variation of the matrix and fibers are plotted in Figs. 5 and 6, respectively, and it can be seen that the density attenuation region extends deeper along the thickness direction of the material structure with ablation time. The density gradient in the region near the heating surface is larger compared to other regions, thereby indicating that the C/C composite undergoes a larger density reduction near the heating surface. This phenomenon can be attributed to the higher temperature in the area near the heating surface resulting in a more pronounced thermal decomposition in this region. Additionally, during

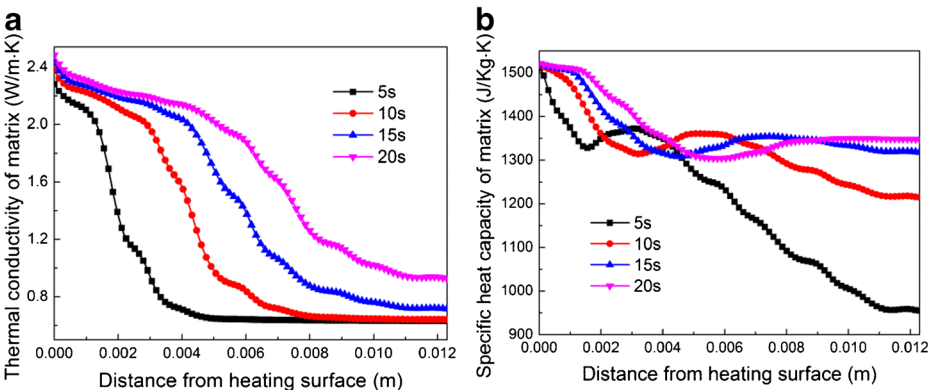


**Fig. 9** Thermal conductivity (a) and specific heat capacity (b) of the matrix along the thickness direction



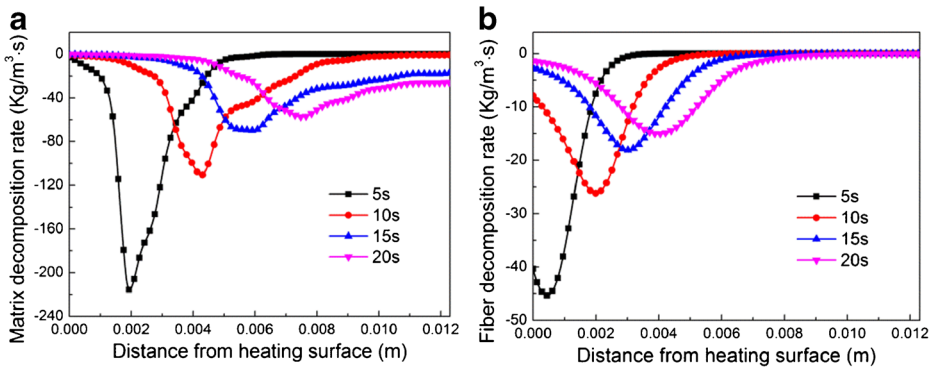


**Fig. 10** Decomposition rates of the (a) matrix and (b) fibers along the thickness direction

ablation, the matrix density is reduced by 59.7% near the heating surface, while the fibers only undergo a 15.9% density reduction within 20 s.

The average fiber density during ablation (Fig. 7) shows a relatively small reduction (4.5% reduction in 20 s) compared to that of the matrix (40.1% reduction with an almost linear decrease with ablation time), suggesting that the matrix undergoes a more pronounced thermal decomposition process, losing more mass during ablation in relation to the fibers.

The C/C composite matrix shows higher values of thermal conductivity and specific heat capacity near the heating surface in relation to the bulk during ablation (Figs. 8 and 9), thus indicating a hindered heat flow towards the bulk of the material and resulting in a heat concentration mainly in the area near the heating surface; this is a major characteristic of the C/C composite, important in avoiding the internal structure fatigue at relatively high temperatures. Furthermore, as the ablation time increases, the overall values of thermal conductivity and specific heat capacity also increase, indicating that the thermal resistance of the C/C composite gradually decreases. Therefore, the heat conduction ability is significantly enhanced through the ablation process.

The decomposition rates of the matrix and fibers under ablation conditions (i.e., the thermal decomposition speed of the ablation process), occur at varying distances at different times (Fig. 10), showing local peaks. At these local peak times, the material decomposes most intensely. The position of the peak shifts to greater distances from the heating surface and the absolute value of the peak decreases with ablation time, mainly due to the gradual decrease of temperature along the

**Fig. 11** Mass loss during ablation as a function of ablation time

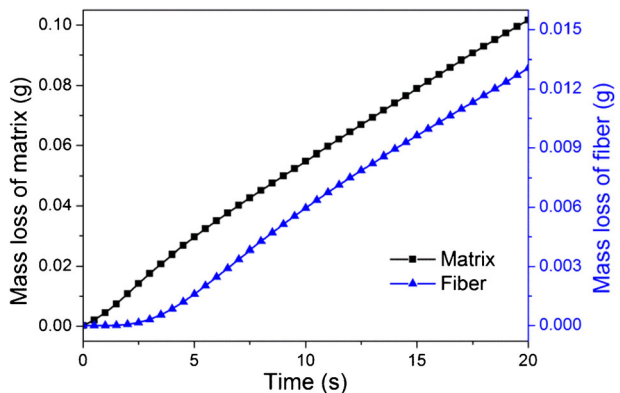
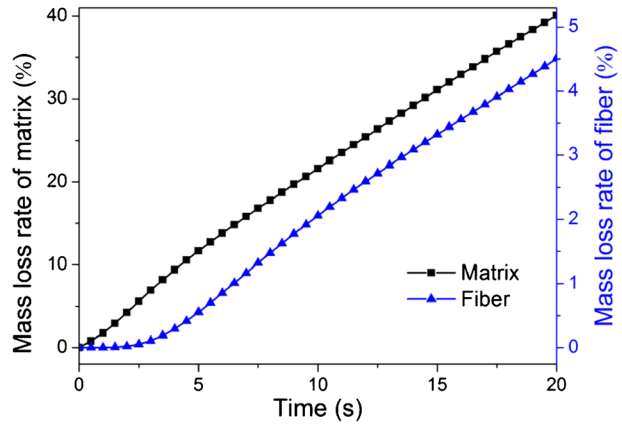


**Fig. 12** Mass loss rate during ablation as a function of ablation time



thickness direction during ablation. Additionally, the matrix decomposition rate is noticeably larger than that of the fibers during ablation.

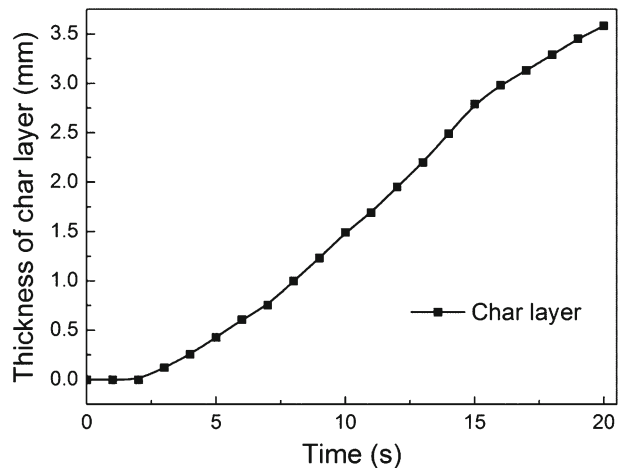
The mass loss and mass loss rate of the C/C composite during ablation (Figs. 11 and 12, respectively) show that the matrix undergoes considerable mass loss during ablation, while changes in fiber mass are minimal. The mass loss rate of the matrix reaches 40% at 20 s, while that of the fibers reaches only 4.5% over the same time period. Therefore, the C/C composite matrix undergoes more serious erosion than the fibers during ablation.

With the decomposition of the internal material, a porous char layer is produced during ablation. The matrix char layer at the initial stage of the ablation is practically nonexistent (Fig. 13), but gradually increases with ablation time, such that, at 20 s, the char layer thickness reaches 3.58 mm.

## 4 Conclusion

Based on energy- and mass-conservation principles and the coupling thermal decomposition equation, an ablative model for a thermoprotective 4D C/C composite is utilized

**Fig. 13** Thickness of char layer during ablation as a function of ablation time



herein to simulate the composite's thermal response in the volume ablation process. The temperature distribution, density, thermal conductivity, specific heat capacity, mass loss, and char layer thickness are quantitatively calculated under ablation conditions.

During the ablation process, the maximum surface temperature reaches 2129 K in 20 s, and the matrix temperature on the heating surface is significantly higher than the fiber temperature, with the temperature difference reaching 246 K. The matrix is observed to undergo a more pronounced decomposition process, and the average matrix density is reduced by 40.1%, with an almost linear decrease with ablation time. As the ablation time increases, the overall values of thermal conductivity and specific heat capacity of the matrix increase, indicating that the thermal resistance of the C/C composite gradually decreases and the heat conduction ability is significantly enhanced with ablation. The decomposition rates of the matrix and fibers show local peaks during ablation, with a peak shift towards greater distances from the heating surface and the absolute value of the peak decreasing with ablation time.

## References

1. Fitzer, E.: The future of carbon-carbon composites. *Carbon*. **25**, 163–190 (1987)
2. Amada, S., Wu, Y.N., Qi, Z.M., Akiyama, S.: Thermal shock resistance of carbon-carbon (C/C) composite by laser irradiation technique. *Ceram. Int.* **25**, 61–67 (1999)
3. Lu, J., Hao, K., Liu, L., Li, H., Li, K., Qu, J., Yan, X.: Ablation resistance of SiC-HfC-ZrC multiphase modified carbon/carbon composites. *Corros. Sci.* **103**, 1–9 (2016)
4. Borie, V., Brulard, J., Lengelle, G.: Aerothermochemical analysis of carbon-carbon nozzle regression in solid-propellant rocket motors. *J. Propuls. Power.* **5**, 665–673 (2012)
5. Thakre, P., Yang, V.: Chemical Erosion of Carbon-Carbon/Graphite Nozzles in Solid-Propellant Rocket Motors. *J. Propuls. Power.* **24**, 822–833 (2008)
6. Bianchi, D., Nasuti, F.: Thermochemical Erosion Analysis of Carbon-Carbon Nozzles in Solid-Propellant Rocket Motors. Proc. 46th AIAA/ASME/SAE/ASEE Joint Propulsion Conference & Exhibit, AIAA paper no. 2010–7075, Nashville, TN (2010)
7. Lachaud, J., Vignoles, G.L.: A Brownian motion technique to simulate gasification and its application to C/C composite ablation. *Comput. Mater. Sci.* **44**, 1034–1041 (2009)
8. Lachaud, J., Aspa, Y., Vignoles, G.L.: Analytical modeling of the steady state ablation of a 3D C/C composite. *Int. J. Heat Mass Transf.* **51**, 2614–2627 (2008)
9. Vignoles, G.L., Lachaud, J., Aspa, Y., Goyh  n  che, J.M.: Ablation of carbon-based materials: multiscale roughness modelling. *Compos. Sci. Technol.* **69**, 1470–1477 (2009)
10. Duffa, G., Vignoles, G.L., Goyh  n  che, J.M., Aspa, Y.: Ablation of carbon-based materials: Investigation of roughness set-up from heterogeneous reactions. *Int. J. Heat Mass Transf.* **48**, 3387–3401 (2005)
11. Martin, A.: Volume averaged modeling of the oxidation of porous carbon fiber material. Proc. 44th AIAA Thermophysics Conference, AIAA paper no. 2013–2636, San Diego, CA (2013)
12. Panerai, F., Mansour, N.N., Lachaud, J., Martin, A.: Experimental and Numerical Study of Carbon Fiber Oxidation, Proc. 52nd Aerospace Sciences Meeting, AIAA paper no. 2014–1208, National Harbor, Maryland (2014)
13. Lachaud, J., Eekelen, T.V., Scoggins, J.B., Magin, T.E., Mansour, N.N.: Detailed chemical equilibrium model for porous ablative materials. *Int. J. Heat Mass Transf.* **90**, 1034–1045 (2015)
14. Lachaud, J., Mansour, N.N.: Porous-Material Analysis Toolbox Based on Open FOAM and Applications. *J. Thermophys. Heat Transf.* **28**, 191–202 (2014)
15. Lachaud, J., Scoggins, J.B., Magin, T.E., Meyer, M.G., Mansour, N.N.: A generic local thermal equilibrium model for porous reactive materials submitted to high temperatures. *Int. J. Heat Mass Transf.* **108**, 1406–1417 (2017)
16. Schroyen, P., Hillewaert, K., Magin, T.E., Chatelain, P.: Fully implicit Discontinuous Galerkin solver to study surface and volume ablation competition in atmospheric entry flows. *Int. J. Heat Mass Transf.* **103**, 108–124 (2016)
17. Ferguson, J.C., Panerai, F., Lachaud, J., Martin, A., Bailey, S.C.C., Mansour, N.N.: Modeling the oxidation of low-density carbon fiber material based on micro-tomography. *Carbon*. **96**, 57–65 (2016)
18. Li, W., Huang, H., Xu, X.: A coupled thermal/fluid/chemical/ablation method on surface ablation of charring composites. *Int. J. Heat Mass Transf.* **109**, 725–736 (2017)

19. Li, W., Huang, H., Wang, Q., Zhang, Z.: Protection of pyrolysis gases combustion against charring materials' surface ablation. *Int. J. Heat Mass Transf.* **102**, 10–17 (2016)
20. Li, W., Huang, H., Tian, Y., Zhao, Z.: Nonlinear analysis on thermal behavior of charring materials with surface ablation. *Int. J. Heat Mass Transf.* **84**, 245–252 (2015)
21. Li, W., Huang, H., Ai, B., Zhang, Z.: On the novel designs of charring composites for thermal protection application in reentry vehicles. *Appl. Therm. Eng.* **93**, 849–855 (2016)
22. Scoggins, J.B., Mansour, N.N., Hassan, H.A.: Development of a Reduced Kinetic Mechanism for PICA Pyrolysis Products. Proc. 42nd AIAA Thermophysics Conference, AIAA paper no. 2011–3126, Honolulu, Hawaii (2011)
23. Scoggins, J.B., Hassan, H.A.: Pyrolysis Mechanism of PICA, AIAA paper. Proc. 10th AIAA/ASME Joint Thermophysics and Heat Transfer Conference, AIAA paper no. 2010–4655, Chicago, Illinois (2010)
24. Aghaaliakbari, B., Jaid, A.J., Zeinali, M.A.A.: Computational simulation of ablation phenomena in glass-filled phenolic composites. *Iran. J. Chem. Chem. Eng.* **34**, 97–106 (2015)
25. Shi, S., Li, L., Fang, G., Liang, J., Yi, F., Lin, G.: Three-dimensional modeling and experimental validation of thermomechanical response of FRP composites exposed to one-sided heat flux. *Mater. Des.* **99**, 565–573 (2016)
26. Shi, S., Li, L., Liang, J., Tang, S.: Surface and volumetric ablation behaviors of sifrp composites at high heating rates for thermal protection applications. *Int. J. Heat Mass Transf.* **102**, 1190–1198 (2016)
27. Gibson, A., Browne, T., Feih, S., Mouritz, A.: Modeling composite high temperature behavior and fire response under load. *J. Compos. Mater.* **46**, 2005–2022 (2012)
28. Yin, T., Zhang, Z., Li, X., Feng, X., Feng, Z., Wang, Y., He, L., Gong, X.: Modeling ablative behavior and thermal response of carbon/carbon composites. *Comput. Mater. Sci.* **95**, 35–40 (2014)
29. Wang, C.: Numerical analyses of ablative behavior of C/C composite materials. *Int. J. Heat Mass Transf.* **95**, 720–726 (2016)
30. Wang, C., Liang, J., Wu, S., Du, S.: Numerical simulation of c/c composites coupled thermo-mechanical field under the condition of high temperatures and ablation. *Acta Mater. Compos. Sin.* **23**, 143–148 (2006)
31. Meng, S., Zhou, Y., Xie, W., Yi, F., Du, S.: Multiphysics coupled fluid/thermal/ablation simulation of carbon/carbon composites. *J. Spacecr. Rockets.* **53**, 930–935 (2016)
32. Riccio, A., Damiano, M., Zarrelli, M., Giordano, M., Scaramuzzino, F.: Simulating the Response of Composite Plates to Fire. *Appl. Compos. Mater.* **21**, 511–524 (2014)
33. Sanoj, P., Kandasubramanian, B.: Hybrid Carbon-Carbon Ablative Composites for Thermal Protection in Aerospace. *J. Compos.* **2014**, 1–15 (2014)
34. Riccio, A., Damiano, M., Zarrelli, M., Scaramuzzino, F.: Three-dimensional modeling of composites fire behavior. *J. Reinf. Plast. Compos.* **33**, 619–629 (2014)